PCCP

Accepted Manuscript

ROYAL SOCIETY OF CHEMISTRY

www.rsc.org/pccp

Journal Name

RSCPublishing

ARTICLE

Silicon-pyrenes/ perylenes hybrids as molecular rectifiers

Cite this: DOI: 10.1039/xoxxoooooox

Received ooth January 2012,
Accepted ooth January 2012

DOI: 10.1039/xoxxoooooox

www.rsc.org/

Kavita Garg [a], Chiranjib Majumder [b], Sandip K. Nayak [a], Dinesh K. Aswal [c], Shiv K. Gupta [c] and Subrata Chattopadhyay [a *]

*We have synthesized two alkenyl (C-6 and C-11 chains) pyrenes and one alkenyl (C-11 chain) perylene as the σ–π systems, which were electro-grafted on H-terminated Si surfaces to form the respective monolayers. The I–V characteristics of the monolayers revealed pronounced rectification in forward bias with maximum rectification ratio (RR) of 2.5 × 10^5 at 2.5 V for the C-6-pyrene **4b**, 1000 at 1.5 V for the C-11-pyrene **4a** and 3000-5000 at 1.75 V for the C-11-perylene **3**. The higher RR of the devices containing **4b** compared to those of **4a** and **3** is possibly due to better alignment and packing of the **4b**-monolayers on Si substrate. The rectification was explained using the ab initio molecular-orbital calculations.*

Introduction

Nonlinear charge transport in organic molecules grafted on Si is a key research area in hybrid nanoelectronics such as molecular diodes, resonant tunnel diodes, molecular transistors etc.[1-3] Supramolecular assembly of organic molecules on solid substrates is a powerful `bottom-up' approach for the fabrication of devices for molecular-scale electronics. This is generally achieved by forming Langmuir-Blodgett (LB) films,[4] or self-assembly of monolayers (SAM) of organic molecules on solid substrates via metal/molecules/metal (MMM) junctions.[5] However, chemically-grafted organic molecules on semiconductors like Si is most promising for this purpose because the surface potential can be tailored to develop improved hybrid molecular devices.[3] The p-n junction threshold voltage for rectification can be adjusted by changing the electronic nature of the organic π group molecules, instead of the classical doping method.

Molecules, showing rectification behaviour with high rectification ratio (RR) is very useful for making rectifying diodes. Several groups including us have shown rectification behaviour of σ–π systems grafted on Si through an alkyl spacer (σ).[6-8] The rectification property is due to a resonant transport between the Si conduction band (CB) and the highest occupied molecular orbital (HOMO) of the π group. The Fermi level pinning at the metal/ π-group interface plays a key role in the electrical behavior of these molecular rectifying junctions. One of the challenges in this area is to develop devices that are environmentally stable, have high electron mobility and are easily processable. Due to their high ionization energies and band gaps, the perylenes/pyrenes are suitable π−moieties for making rectifying diodes, and several such systems have been constructed.[9-12] Attachment of the alkyl (σ) moiety to the polyaromatic hydrocarbons (PAHs) including the perylenes improved their solubility enormously.[13-15] Besides LB films, chemically bonded monolayers on Si surfaces can be prepared either on Si oxide (SiOx) surfaces through silane chemistry or on oxide-free Si.[16,17] The Si−based SAMs are better because of better Si−molecule electronic coupling and lack of charging effect, observed with native/ thin SiOx layers. Several thoughtful reviews by Cahen and his group dealing with in-depth analysis of different fabrication methods for Si/SAM/Hg junctions, relative advantages and limitations of these methods and characterization of SAMs on H-terminated Si are available.[18,19] Hydrosilysation of Si-H surfaces with alkenes/alkynes can be achieved by activating the Si-H bond with heat,[20] light[21,22] and electrochemistry,[23,24] or using Lewis acids,[25] radical initiators,[26] or via Grignard route.[27] Many of these protocols provide densely packed SAMs with high surface coverages. Due to the very high Si atom surface

density on the Si(111) surface, the longer alkyl chains generally provide SAMs with less surface coverages (≤50%), leaving the rest of the surface unmodified.

For the past several years, our group is actively engaged in fabricating chemically-bonded organic molecules on H-terminated Si surfaces for molecular electronics applications.[28] To this end, the present work was carried out to explore the potential of the organo-Si hybrids using alkenylpyrene/ perylene as the σ–π molecules. Grafting of a ω-functionalized alkenes followed by a late-stage attachment of suitable PAH derivatives would be ideal to obtain compact monolayers. Indeed, this strategy has been extensively used for attaching electroactive aryl moieties through ester or amide linkages.[29,30] In some cases the alkyl-Si precursor, containing both non-functionalized and ω-functionalized platform was used for better surface coverage of some ferrocenes.[30] However, direct attachment of the large electroactive organic moieties using preformed ω-arylalkenes remains by and large unexplored except in some rare cases.[31,32] We intended to use the large electroactive PAHs attached to the alkyl moiety via the ether linkage that is chemically more stable than the ester/amide bonds. For this, the late-stage functionalization may be unsuitable, because the chemistry of attaching the organic molecule at the alkyl group will be cumbersome. Moreover, the steric bulk of the PAHs would not allow a good attachment yield of the PAHs, resulting in SAMs containing an undefined mixture of only alkyl and PAH-alkyl groups on the Si surface. Hence, we used pre-synthesized alkenylpyrene/ perylene molecules for electro-grafting the monolayers on H-terminated Si (111) wafers, characterized them, and investigated their current rectification behaviour. The cathodic electrografting has some distinct advantages: (i) the process is very easy; (ii) its completion can be monitored online; and (iii) the negative potential, applied to the Si substrates excludes the possibility of oxidation and/or hydrolysis at the Si surfaces. This strategy was expected to give uniformly layered alkylpyrene/ perylene monolayers on Si, albeit with less compactness (*vide infra*). Thus, we synthesized the monolayers of two alkenylated pyrenes and one perylene derivative on H-terminated Si (111) wafers. *I–V* characteristics of the hybrid systems revealed stable and reproducible rectification property. We also demonstrate tuning the rectification property by subtle changes in alkyl chain lengths that controlled the packing of the monolayers on the Si surface.

Results and Discussion

Synthesis of the pyrene and perylene derivatives

To synthesize the alkyl perylene **3**, we first attempted an $AlCl_3$-catalyzed Friedel-Crafts acylation of perylene at its most electrophilic C-3 centre with 10-undecenoyl chloride, prepared by reaction of 10-undecenoic acid with $SOCl_2$. However, the reaction gave a mixture of mono- and di-acyl perylenes along with the starting compound. In view of the poor solubility of the reaction products, their separation was difficult.[33] Hence we adopted an alternative strategy, wherein the electron-rich perylene was regioselectively formylated at its C-3 position by the Vilsmeier-Haack reaction to obtain compound **1**. Its $NaBH_4$ reduction in THF gave the alcohol **2**, which on *O*-alkylation with 11-bromoundec-1-ene using NaH as the base gave the desired product **3** (Scheme 1). The required electrophile, 11-bromoundec-1-ene was synthesized by $LiAlH_4$ reduction of the inexpensive 10-undecenoic acid followed by bromination with Ph_3P/Br_2 in the presence of pyridine.[34] For synthesizing the alkyl pyrenes **4a** and **4b**, commercially available 1-pyrenemethanol was subjected to a base-catalyzed *O*-alkylation with suitable ω-bromoalkenes (Scheme 2).

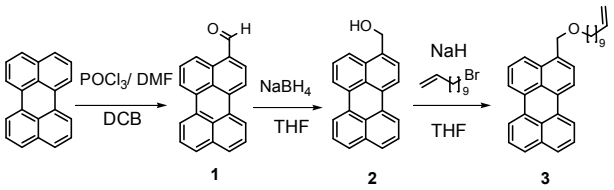

Scheme 1. Synthesis of compound **3**.

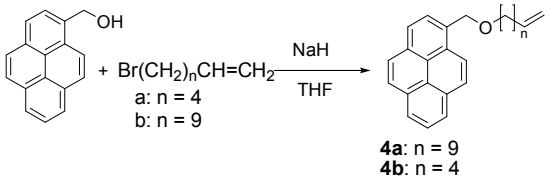

Scheme 2. Synthesis of compounds **4a** and **4b**.

Preparation of the Si-hybrids

The cyclic voltammograms (CVs) (Fig. 1), recorded during electrochemical deposition of molecules **3**, **4a**, and **4b** on the H-terminated Si surfaces showed an irreversible peak at ~0.3 V, indicating covalent attachment of the molecules at the Si surfaces. A similar peak was observed with 1-undecene (SL-1), but not with the blank **(**only electrolyte). As the number of scans increased, the peak diminished owing to the non-availability of nucleophilic Si atoms on the surface. Using different number of scans (5, 10, 20, 25, 30 and 50), formation of the respective monolayers were optimized. Compounds **3** and **4a** required 50 scans, while **4b** required only 20 scans to form the compact monolayers, as revealed by AFM (Fig. 2). Formation of multilayers at higher scans was evident by AFM analysis (data not shown).

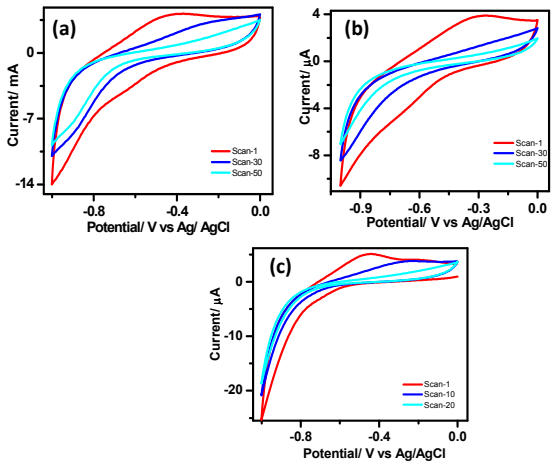

Figure 1. CVs indicating electrografting of the molecules on silicon (n^{++}) wafers. (a) **3**; (b) **4a**; (c) **4b**. The deposition was carried out under N_2 atmosphere at a scan rate of 0.05 V/s using Si wafers as the WE, Pt as the CE, Ag/AgCl as the RE, 0.1 M Bu_4NP as the electrolyte and the pyrenes/perylenes (1 μM) in dry CH_2Cl_2.

Characterization of the monolayers The contact angles of deionized water in case of Si wafers, grafted with **3**, **4a**, and **4b** were 68°, 74° and 80° respectively, whereas these were 84° for the cleaned H-terminated Si wafers and 112° for the C-11 alkyl-grafted Si surface. Our data are consistent with a previous report, where monolayers of functionalized 1-alkenes on Si substrate showed significantly lower water contact angles (advancing and receding: 73-85°/65-73°) than that of the highly ordered alkene-Si monolayers (109-110°/94-96°).[20] The low contact angles of the present monolayers revealed them to be less compact or more disordered than the alkane-Si monolayers. Because we used aryl-terminated alkyl moiety for grafting, the reduction of contact angles was expected. The observed contact angles are in close proximity with the contact values (66-74°) reported for the -COO-pyrene- and thiophene-terminated alkyl monolayers on Si surfaces that were prepared by a late-stage attachment of the aryl moieties.[29,31] This established the suitability of our direct attachment protocol for the preparation of the monolayers. The low contact angles of the monolayers suggested them to be tilted on the surface that would expose the ether oxygen to interact with water droplets.

Our ellipsometry data revealed that the average thicknesses of respective monolayers were 2.4 ± 0.1 nm for **3**, ~1.9 ± 0.2 nm for **4a** and 1.2 ± 0.1 nm for **4b**. But the lengths of theoretically optimized **3**, **4a** and **4b** molecules were 2.7, 2.1 and 1.4 nm respectively. Taken together, these data confirmed that our monolayers were tilted with the calculated tilt angles as 58.3°, 58.9° and 54.3° for the respective monolayers of **3**, **4a** and **4b**. This is much more than the tilt angles (26-29°), reported for simple alkyl monolayers on Si (100) surfaces.[20] The bulky aryl groups at the termini of our monolayers may account for this.

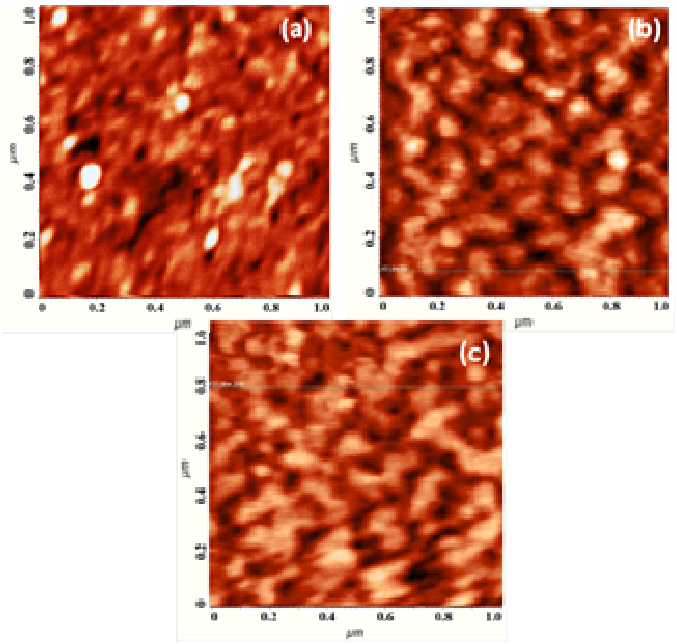

Figure 2. AFM images (1 μm × 1 μm) for the monolayers of (a) **3**; (b) **4a**; (c) **4b**, electro-grafted on silicon (n^{++}) wafers.

Consistent with our low contact angle data, the AFM images also suggested that the monolayers of **3**, **4a**, and **4b** were less compact. Nevertheless, the monolayers of **4a** and **4b**, but not of **3** had definite patterns of orderly packing due to molecular stacking through van der Waal's interactions. The monolayers of **4b** were more compact and uniform with larger grain size, compared to that of **4a**. However, possibly due to non-planarity of perylene, the monolayers of **3** were scattered without any definite pattern. The RMS roughness and average roughness values of the monolayers were 0.39 and 0.28 nm for **3**, 0.52 and 0.43 nm for **4a**, and 0.41 and 0.33 nm for **4b**. In a previous report, the rms roughness was found to increase on attaching the pyrene group at the preformed alkyl-Si monolayer, due to the larger size of the pyrene moiety compared to the terminal methyl group. For example, the rms roughness for the HETS pyrene SAMs was ~0.22 nm and they displayed void depths of about 0.5-0.7 nm.[29] The void depths of the monolayers were 2.3 nm for **3**, 1.8 nm for **4a** and ~ 1.3 nm for **4b** (Fig. 2 and SL-2). Overall, the AFM data suggested that amongst the monolayers, those of **4b** were relatively more organized with least number of voids and hillocks.

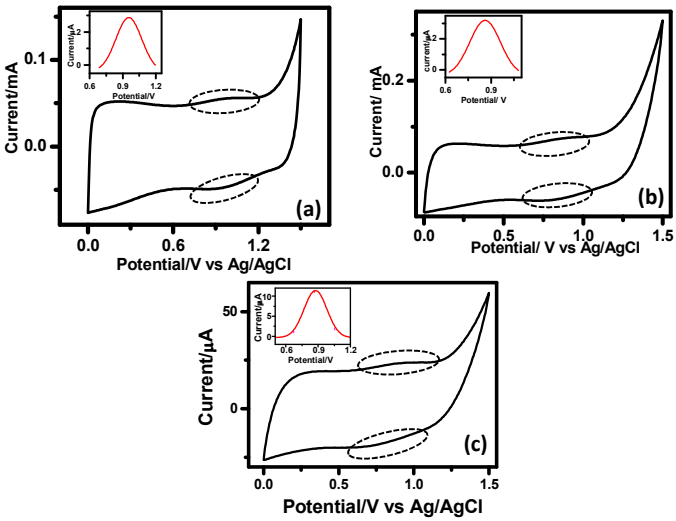

Figure 3. Fast scan CVs for the monolayers of (a) **3**; (b) **4a**; (c) **4b**, electro-grafted on silicon (n^{++}) wafers. The CVs were recorded under N_2 atmosphere at a scan rate of 10 V/s using the respective monolayer-grafted Si as the WE, Pt as the CE and Ag/AgCl as the RE, and 0.1 M Bu_4NP as the electrolyte. The reversible peaks are indicated by circles. Insets show the magnified redox peaks, after background correction.

The fast scan (10 V/s) CVs of the respective monolayers (Fig. 3) exhibited a reversible peak at +0.8 V, typical for the electron-rich PAH moieties. No such peak was observed for the blank Si samples and the C-11 alkyl monolayers. The net charge transferred during the oxidation process, calculated from the areas under the oxidation peaks were 3.62×10^{-8}, 3.5×10^{-8} and 1.72×10^{-6} C respectively for **3**, **4a** and **4b**. These amounted to the surface coverages [surface coverage = total charge / (F × area dipped in electrolyte)] of 2.52×10^{11}, 5.62×10^{12} and 1.59×10^{13} molecules/cm^2 for **3**, **4a** and **4b**. Hence the areas occupied by **3**, **4a** and **4b** were 396.82, 17.78 and 6.29 nm^2/molecule respectively. This is much higher than that (24 Å^2/molecule) reported for the monolayers of simple C_{18}-, C_{16}-, and C_{12}- alkanes on Si (100).[20] In case of **3**, the area occupied by each molecule was the highest, reflecting poor ordering of its monolayers. This may be because of poor π–π stacking of the non-planar perylene moiety. In case of **4a** and **4b**, the area occupied by each molecule is comparatively less because of

better π–π stacking of the planar pyrene moieties. Because the shorter alkyl chain in **4b**, its monolayers were better ordered and the surface coverage was ~ 2.8 times that of **4a**, containing a longer alkyl moiety. These data are consistent with the AFM analyses, both revealing more compact monolayers with **4b** than **4a**. Our XPS data (SL-3) showed absence of SiO_2 peak at 103 eV, and presence of a peak at 99.5 eV due to the Si-C bond in the monolayers, confirming that the monolayers were free from SiO_2.

The SIMS of the monolayers of **3** showed peaks due to the perylene fragments at 310, 295, 285, 270 and 258 (Fig. 4 (a)). In case of the compound **4a**, the peaks due to the pyrene fragments appeared at m/z 244, 206, 184, 147, 142 and 116 amu (Fig. 4 (b)). But the peaks appeared at a lower mass range *viz*. at m/z 215, 181, 164 and 114 amu (Fig. 4 (c)) with compound **4b**. These confirmed the deposition of the monolayers on the Si surfaces. The monolayers of **3** and **4a** with C-11 alkyl chains showed the largest mass fragment at m/z 310 and 244 amu respectively. Considering the molecular weight of 1-pyrenemethanol as 232 amu, these peaks can be assigned to ([perylene-$CH_2OCH_2CH_2$]-1) and ([pyrene-CH_2OCH_2]-1] units respectively. Compound **4b** with a shorter (C-6) alkyl chain showed a smaller fragment at m/z 215 corresponding to the [pyrene-CH_2] unit.

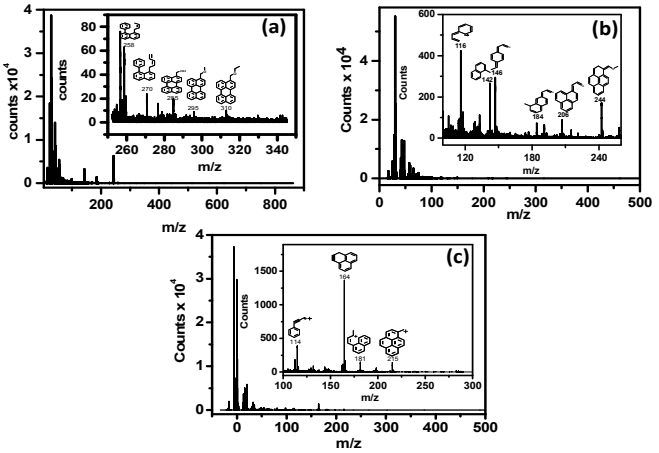

Figure 4. SIMS of the monolayers of (a) **3**; (b) **4a**; (c) **4b**, electro-grafted on silicon (n^{++}) wafers.

In pure solid alkene monolayers, the hydrocarbon chains exist in an all-*trans* configuration such that the carbon backbone of each molecule lies in a single plane to maximize the enthalpy gain (~ 2 kcal/mol per CH_2 unit).[35,36] However, in liquid form, there is substantial twisting about the individual bonds. These out-of-plane twists alter the frequency of the CH_2 vibrational modes.[20,37] Thus, the IR peaks due to the CH_2 vibrational modes provide good insights about the van der Waals interactions. The polarized FTIR spectra (Fig. 5) for the monolayers showed that with compound **4a**, the symmetric (ν_s) and asymmetric stretching (ν_a) CH_2 vibrations appeared at 2853 and 2923 cm^{-1}. In contrast, the respective IR absorption peaks of the monolayers of **4b** were observed at 2847 and 2920 cm^{-1}. These suggested that the alkyl chains in the monolayers of **4b** (containing a C_6-alkyl unit) are more rigid like in pure solid alkanes, while that in the monolayers of **4a** (containing a C_{11}-alkyl unit) are twisted *i. e*., more liquid like. In other words, there is an increase in the van der Waals interactions between neighboring molecules in case of the **4b** monolayers compared to that with **4a**. In case of the perylene derivative **3**, the ν_s and ν_a CH_2 vibrations also appeared at 2853 and 2926 cm^{-1}, indicating twisted monolayers. The IR data of the **4a** monolayers were comparable to those reported in photochemical grafting of 1-octene[38] and chemical grafting of simple C_{12}-C_{18} alkenes to Si surfaces.[20]

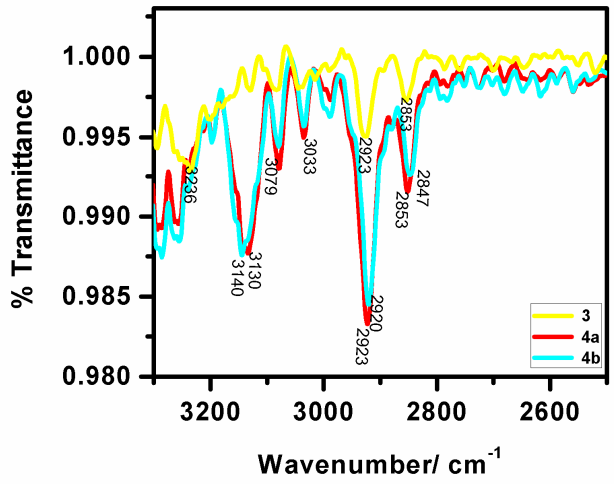

Figure 5. Polarized FTIR of **3, 4a** and **4b**-grafted monolayers on silicon (n^{++}) wafers.

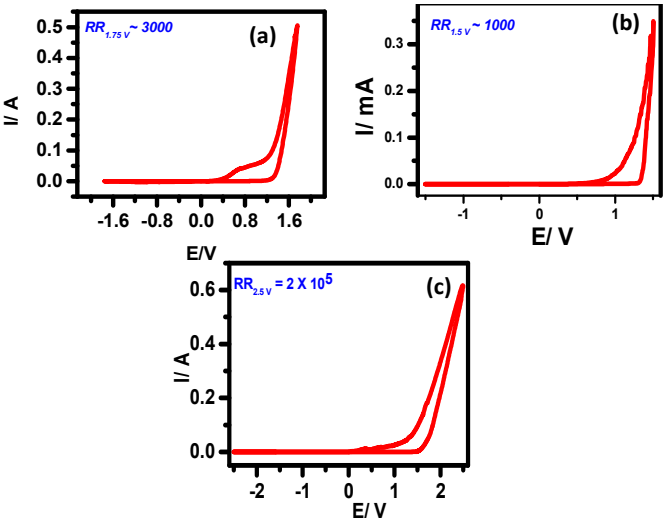

Figure 6. *I-V* characteristics of Hg/ molecules grafted monolayers/Si(n^{++}) devices. (a) **3**; (b) **4a**; (c) **4b**. The *I-V* characteristics of the device samples, made from the same molecules were similar, and typical curves are shown.

I-V characteristics

The *I-V* curves of Hg/ molecule/ Si (111) wafers, recorded at a scan rate of 0.01V/s are shown in Fig. 6. Control experiments, carried out with blank as well as C-11 alkyl chain-grafted Si-wafers showed nearly symmetrical sigmoidal *I-V* curves (SL-4). All the devices showed current rectification in the forward bias. The device made of the C-6 alkylated pyrene moiety **4b** showed excellent results with the maximum rectification ratio (RR) of 2–5 × 10^5 at 2.5 V due to compact packing as compared to that with the C-11 alkylated pyrene (**4a**)-based device (maximum RR ~ 1000 at 1.5 V). The maximum RR observed with the device made of the perylene derivative **3** was 3000-5000 at 1.75 V. The rectification in the forward bias was due to the resonance tunnelling through HOMO of the molecules at bias >

1 V. Molecular stacking is very important for the electrical behaviour of the organic semiconductors, as overlapping of electrons clouds favours the generation and transport of charge carriers to induce intrinsic conductivity. Our AFM results indicated larger defects in the monolayers of **3** and **4a** than that in **4b**. This may be due to the longer alkyl bridge in the molecules **3** and **4a**, compared to that in **4b**.[39] Consequently, significantly higher maximum RR was observed with the **4b** monolayers. All the systems were stable during repetitive voltage scanning up to 15 scans without significant reduction in current or the effect. A gradual drop of RR was observed with all the devices in the subsequent scans. The magnitude of current in the present devices was much higher, raising the device temperature. This might alter the geometry of the molecular assembly, resulting in RR drop.

The control of the organization at the molecular scale is a critical point in performance of devices. Despite being less well ordered, our AFM results showed that void depths (~ 1-2 nm) of the present Si-alkyl//Hg junctions were too small compared to the size of the Hg drops (~ 600 μm). Hence, the Hg drops can't penetrate through the pinholes of the SAMs and the measured *I/V* is expected to be direct. The statistical analyses of data and junction yields are extremely valuable to discriminate artifacts from real data. Amongst the previous reports, Kim et al.,[40] and Nijhuis et al.,[41,42] have employed extensive statistical analyses to assess the performance of their SAM-based devices. Due to the use of a large number of samples, this helped them to identify the true working devices. Such an extensive analysis was beyond the scope of the present work, given that we constructed only 48 devices with each of the compounds **3**, **4a** and **4b**. Nevertheless, we have analyzed the statistics of our *I-V* results as shown in Fig. 7 and Table 1, and summarized in the following.

Table 1. Statistics of *I-V* data

Molecules	No. of samples	No. of devices/ sample	Total no. of devices	Devices exhibiting Rectification
3	6	8	48	48
4b	6	8	48	48
4a	6	8	48	48

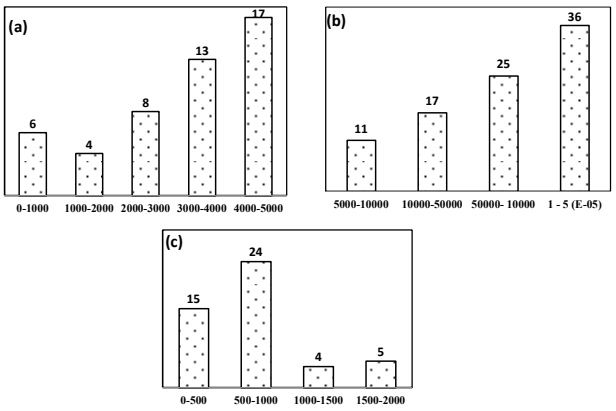

Figure 7. Statistics of rectification ratios of the devices. (a) **4a**; (b) **4b**; (c) **3**. The figures reflect the numbers of devices showing different RR ranges, shown in the X-axes.

With compound **3**, the RR values of a majority (63%) of the devices were 3000-5000, while 25% of the devices showed RR values 1000-3000, the rest showing RR values 500-1000. With compound **4a**, only 10% and 8% of the devices showed RR values of 1500-2000 and 1000-1500 respectively. Fifty percent devices had RR values of 500-1000, and the rest had even lesser (100-500) RR values. The device statistics of the monolayers of **4b** was very impressive with 36% of the devices showing RR values of ~10^5, an additional 42% with RR ≥ 10000, and the rest with RR ≥ 5000. Overall, all the devices, made of the compounds **3**, **4a** and **4b** showed current rectification behavior, and their performance was superior to many of the rectifiers reported so far. This is reflected from RR values (Table 2) of some of the MMM junctions prepared earlier.

Table 2. Current rectification by few reported MMM junctions

Organic-inorganic hybrids	RR values	Ref.
Si/alkyl-Ar(phenyl/thiophene/pyrene ter-thiophene)/Al	35 at -1 V	12
Au/5-(4-dibutylaminobenzylidene)-2-octadecyl-5,6,7,8-tetrahydro isoquinolinium octadecylsulfate LB/Au	70 at 1 V	43
Au/1-butyl-2,6-bis[4-(dibutylamino)styryl] pyridinium iodide/Au	90 at 1 V	44
Au/dimethylanilino-aza[C60]-fullerene/Au	2×10^4 at 1 V	45
Au/*N*-(10-nonadecyl)-*N*-(2-ferrocenyl-ethyl)-pyrenyl-methyl)perylene-3,4,9,10-bis(dicarboxy-imide)/Au	30 at 1 V	46
Au-S-$C_{10}H_{20}$-A^+-π-D|D^-|Au A^+ = 5-(4-dimethylaminobenzylidene)-5,6,7,8-tetrahydro-isoquinolinium Counterion = copper phthalocyanine-3, 4',4",4"'-tetrasulfonate	3000 at 1 V	47
Au/S-$C_{10}H_{20}CuPc(SO_3^-)_4$ salt of 4-[2-(4-dimethylaminonaphthalen-1-yl)-vinyl]-quinolinium/Au	900 at 1 V	47
Hg/tetra-(4-flurophenyl)porphyrin/C60/ Si diodes	1500 at -1 V	48

Theoretical calculations

The rectification behavior of SAMs is because of the resonant tunneling through one of the MO's of the molecules, which is due to the geometrical asymmetry, energy asymmetry in the positions of the MO's with respect to the Fermi levels of the electrodes and the higher HOMO-LUMO gap, allowing unidirectional current flow.[49,50] In general, the forward bias current flow should be determined by the HOMO states of the molecules, while their respective LUMO states would dictate the reverse bias current. Thus, the rectification in forward bias in case of the pyrenes and perylene is a result of alignment of the HOMO of the molecules with the Fermi-levels of the

electrodes (Fig. 8).[51] To verify this, we have theoretically calculated the HOMO and LUMO energy levels of **3**, **4a**, and **4b** using *ab initio* method (GAMESS software). The geometry optimization without any symmetry constraint was carried out at the B3LYP/6-31G (d,p) level of theory where the exchange correlation functions are expressed using hybrid density functional theory. From the HOMO-LUMO values (Table 3) of the molecules it can be seen that the HOMOs of the molecules are close to the Fermi level of Hg (barrier ~0.6 eV for **3** and ~1.2 eV for **4a** and **4b**). When a forward bias is applied, the Hg Fermi level will go down to be in resonance with the HOMO of the molecule at a particular voltage. This will result in high current due to resonance tunnelling. Presently, the onsets of high current were observed at 0.28 V, 0.78 V and 0.7 V for **3**, **4a** and **4b** respectively, which is consistent with their relative HOMO level energies. Since, the HOMO of **3** (4.89 eV) is very close to the Hg Fermi level (4.3 eV), the resonance occurs at a lower voltage (0.28 V). For **4a** and **4b**, the HOMO values are much higher (~5.5 eV), hence the onset was observed at ≥0.7 V. The LUMOs of the molecules were far away from the Hg Fermi level (barrier ~2.4 for **3** and ~ 2.6 eV for **4a** and **4b**). This does not allow resonance tunneling in the reverse bias. Among all the three monolayers, those of **4b** showed the highest RR. This may be because of better packing between the adjacent monolayers of **4b** and the shorter spacer length in it which makes the flow of current easier in the forward bias.

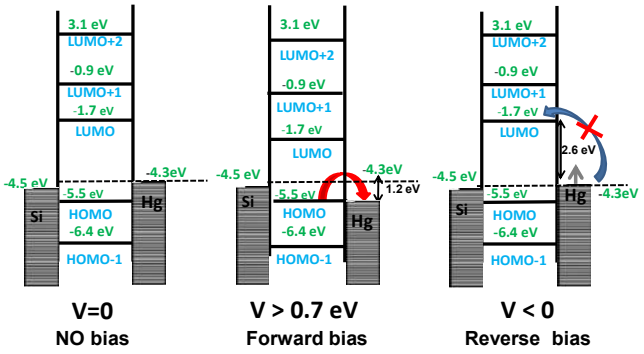

Figure 8. Mechanism of rectification of devices made with **4b**.

Table 3. Theoretically calculated molecular orbital energies for Fig. 7

Molecule	HOMO	LUMO
3	-4.89 eV	-1.877 eV
4a	-5.51 eV	-1.74 eV
4b	-5.52 eV	-1.75 eV

Experimental Section

General

For synthesis of compounds. The chemicals and reagents were purchased from Sigma Aldrich. All solvents were dried and distilled before use. Tetrahydrofuran (THF) and hexane were distilled from Na under argon. DMF was dried over CaH_2 and distilled under vacuum. The ^{1}H NMR and ^{13}C NMR spectra were recorded with 200/300/500 (50/75/100) MHz spectrometers using deuterated solvents as the internal standards. The mass spectrometry was carried out with a MSMS (410 Prostar Binary LC with 500 MS IT PDA Detectors, Varian Inc, USA) and MALDI-TOF/TOF (Bruker Ultraflex II) data systems. The IR spectra were recorded as films with a Jasco model A-202 FT-IR spectrometer and only the pertinent bands are expressed.

For characterization of films. The monolayers were characterized in terms of thickness, using an ellipsometer (Sentech: model SE400 adv); surface morphology by AFM imaging (Multiview 4000, Nanonics), de-ionized water contact angle (Data Physics System, model: OCA20), FT-IR (Bruker, 3000 Hyperion Microscope with Vertex 80 FTIR System, LN-MCT 315-025 detector) in polarized ATR mode (20 × objective) at an angle of 45° for 500 scans and the data are background corrected with freshly prepared Si-H monolayers, and molecular mass by SIMS (BARC make, Kore's Technology software) keeping Si-H as reference. The X-ray photoelectron spectroscopy (XPS) of the deposited films was carried out using a Mg K_α (1253.6 eV) source and a MAC-2 electron analyzer. The XPS analysis chamber was maintained at a base vacuum of 10^{-9} mbar. The XPS binding energy scale was calibrated to Au $4f_{7/2}$ line at 83.95 eV.

Synthesis of 3-formylperylene 1.

Perylene (0.25 g, 1 mmol) was added to a stirred mixture of anhydrous *o*-dichlorobenzene (0.5 mL) and DMF (0.47 g, 6.5 mmol). The reaction mixture was heated to 100 °C and $POCl_3$ (0.31 g, 20 mmol) was added through a dropping funnel over a period of 30 min. After 2 h, the reaction mixture was cooled by an ice bath, and neutralized to Congo red by aqueous 10% NaOAc. After standing in ice for 3 h, the precipitate was collected by filtration, washed with H_2O (3 × 3 mL), dried in air, and purified by column chromatography **(**silica gel, 5% EtOAc/hexane**)** followed by crystallization (hexane/$CHCl_3$) to get **1**. Yield: 0.2 g (71.4%); mp: 235 °C, (lit.[52] mp: 236 °C); IR: 3061, 2718, 1710, 1624 cm^{-1}; ^{1}H NMR ($CDCl_3$, 500 MHz): δ 10.33 (s, 1H), 9.17 (d, *J* = 8.8 Hz, 1H), 8.36-8.24 (m, 5H), 7.94 (d, *J* = 7.8 Hz, 1H), 7.82 (d, *J* = 7.8 Hz, 1H), 7.76 (d, *J* = 7.8 Hz, 1H), 7.70 (t, *J* = 7.8 Hz, 1H), 7.59-7.52 (m, 2H); ^{1}H NMR ($CDCl_3$, 125 MHz): δ 192.8, 137.6, 137.2, 134.4, 132.3, 131.3, 130.7, 130.1, 130.0, 129.9, 129.3, 129.0, 128.5, 128.2, 127.0, 126.7, 124.6, 122.8, 121.6, 121.1, 119.1; LCMS: 281 amu.

Synthesis of 3-hydroxymethylperylene 2.

To a cooled (0 °C) and stirred solution of **1** (0.13 g, 0.46 mmol) in THF (25 mL) was dropwise added $NaBH_4$ (0.018 g, 0.5 mmol) in MeOH (5 mL) in 2 h. The mixture was stirred for an additional 4 h and concentrated in vacuo. The residue was dissolved in $CHCl_3$ (25 mL), the organic extract washed with H_2O (3 × 5 mL) and brine (1 × 5 mL), dried and concentrated in vacuo. The residue was purified by column chromatography (silica gel, $CHCl_3$) followed by crystallization (hexane/$CHCl_3$) to get **2**. Yield: 0.13 g (98%); mp: 207-208°C, (lit.[53] mp: 208-210 °C); IR: 3448, 3063, 1623, 1068 cm^{-1}; ^{1}H NMR ($CDCl_3$, 300 MHz): δ 8.26-8.13 (m, 4H), 7.95 (d, *J* = 8.4 Hz, 1H), 7.69 (d, *J* = 8.1 Hz, 2H), 7.59-7.45 (m, 4H), 5.10 (s, 2H); ^{1}H NMR ($CDCl_3$, 75 MHz): δ 127.9, 126.9, 126.8, 126.7, 126.6, 126.3, 126.1, 126.0, 124.4, 123.4, 120.4, 120.3, 119.8, 63.8; LCMS: 282 amu.

Synthesis of 3-undecenyloxymethylperylene 3.

To a stirred hexane-washed NaH (0.03 g, 1.1 mmol, 60% suspension in oil) suspension in THF (10 mL) was added compound **2** (0.10 g, 0.35 mmol) in THF (10 mL). After refluxing for 1 h, 1-bromo-10-undecene (0.1 mL, 0.42 mmol)

and Bu_4NI (0.1 mmol) was dropwise added into the mixture and the refluxing continued till completion of reaction (*cf*. TLC, ~4 h). The mixture was brought to room temperature, treated with aqueous saturated NH_4Cl (1 mL) and extracted with EtOAc (3 × 15 mL). The organic extract was washed with H_2O (2 × 50 mL) and brine (2 × 10 mL), dried and concentrated in vacuo. The residue was purified by column chromatography (silica gel, 5% EtOAc/ hexane) to give the compound **3**. Yield: 0.12 g (80%); IR: 3231, 988, 920 cm^{-1}; ^1H NMR ($CDCl_3$, 300 MHz): δ 8.26-8.15 (m, 4H), 7.96 (d, *J* = 8.4 Hz, 1H), 7.69 (d, *J* = 8.1 Hz, 2H), 7.57-7.45 (m, 4H), 5.82 (ddt, *J* = 17.0, 10.3, 6.7 Hz, 1H), 5.06-4.86 (m, 4H), 3.58 (t, *J* = 6.6 Hz, 2H), 2.03 (q, *J* = 7.1 Hz, 2H), 1.74-1.55 (m, 4H), 1.40-1.16 (m, 10H); ^{13}C NMR ($CDCl_3$, 75 MHz): δ 139.2, 134.6, 133.8, 133.0, 131.5, 131.3, 131.1, 129.0, 128.5, 127.8, 127.0, 126.6, 126.5, 123.9, 120.3, 120.2, 119.6, 114.1, 71.4, 70.5, 33.8, 29.8, 29.7, 29.6, 29.4, 29.1, 28.9, 26.2; MALDI-TOF *m/z* (%): 434 (100%), 435 (33%); Anal. Calcd. for $C_{32}H_{34}O$: C, 88.43; H, 7.89. Found: C, 88.55; H, 7.94%.

Synthesis of undecenyl 1-methylpyrene ether 4a and hexenyl, 1-methylpyrene ether 4b.

As described for the synthesis of **3**, pyrene-1-methanol (0.20 g, 0.9 mmol) was alkylated with the required bromides (1.0 mmol) using NaH (0.12 g, 5.1 mmol, 60% suspension in oil) as the base in presence of Bu_4NI (0.1 mmol) in THF (15 mL). Isolation of the product followed by purification column chromatography (silica gel, 5% EtOAc/ hexane) gave **4a** and **4b**.

Compound **4a.** Yield: 0.28 g (90%); IR: 3130, 3079, 3033, 1630, 991, 921 cm^{-1}; ^1H NMR ($CDCl_3$, 300 MHz): δ 8.38 (d, *J* = 9.0 Hz, 1H), 8.21-8.10 (m, 4H), 8.06-7.95 (m, 4H), 5.83 (ddt, *J* = 17.1, 10.1, 6.7 Hz, 1H), 5.22 (s, 2H), 5.02-4.89 (m, 2H), 3.59 (t, *J* = 6.4 Hz, 2H), 2.00 (quint, *J* = 6.6 Hz, 2H), 1.65 (quint, *J* = 6.5 Hz, 2H), 1.45-1.19 (m, 12H); ^{13}C NMR ($CDCl_3$, 75 MHz): δ 138.7, 131.7, 131.2, 131.1, 130.8, 129.2, 127.5, 127.3, 127.2, 126.7, 125.8, 125.1, 125.0, 124.8, 124.7, 124.4, 123.4, 114.5, 71.4, 70.3, 33.5, 29.7, 29.4, 29.3, 25.5, 22.7; LCMS *m/z* (%): 383 (100%), 384 (25%), 385 (12.5 %) amu; Anal. Calcd. for $C_{28}H_{32}O$: C, 87.45; H, 8.39. Found: C, 87.77; H, 8.42%.

Compound **4b.** Yield: 0.35 g (90%), IR: 3140, 3079, 3031, 1633, 978, 890 cm^{-1}; ^1H NMR ($CDCl_3$, 200 MHz): δ 8.38 (d, *J* = 9.0 Hz, 1H), 8.31-7.93 (m, 8H), 5.83 (ddt, *J* = 17.0, 10.1, 6.7 Hz, 1H), 5.22 (s, 2H), 5.13-4.91 (m, 2H), 3.63 (t, *J* = 6.4 Hz, 2H), 2.19-2.00 (m, 2H), 1.81-1.47 (m, 4H); ^{13}C NMR ($CDCl_3$, 50 MHz): δ 138.6, 131.7, 131.1, 131.0, 130.7, 129.1, 127.4, 127.2, 127.1, 126.6, 125.7, 125.0, 124.8, 124.6, 124.3, 123.3, 114.4, 71.3, 70.2, 33.4, 29.7, 29.2, 25.5; LCMS *m/z* (%): 231 (100%), 313 (50%), 314 (12.7%) amu; Anal. Calcd. for $C_{23}H_{22}O$: C, 87.86; H, 7.05. Found: C, 87.55; H, 7.39%.

Preparation of H-terminated Si wafers

N-type silicon wafers (orientation: 111; resistivity: 0.001-0.005 Ωcm) and 40% NH_4F were purchased from Siltronix and Fluka, respectively. The Si (111) wafers, cut into small pieces (~ 0.5 cm × 1.5 cm) were cleaned by heating in 3:1 (v/v) of conc. H_2SO_4 : 30% H_2O_2 (piranha) for 10 min at 80 °C. The wafers were washed with excess H_2O and, immersed successively in a deaerated (purged with Ar for 30 min) 40% aqueous NH_4F for 10 min and 2% aqueous HF for 2 min. The wafers were washed with deionized H_2O for 1 min, dried under a stream of N_2 and immediately taken into the electrochemical cell for electro-grafting.

Monolayer formation

The electrochemical deposition of **3**, **4a** and **4b** was carried out by cyclic voltammetry (CV) with a potentiostat/galvanostat system (model: Autolab PGSTAT 30) using the Si wafers as the working electrode (WE), Pt as the counter electrode (CE) and Ag/AgCl as the reference electrode (RE). The solution contained 0.1 M Bu_4NP as the electrolyte and **3**, **4a** or **4b** (1 μM) in dry CH_2Cl_2. The CV was run from 0 to -1 V for 25-50 cycles at 0.05 V/s scan rate under an inert atmosphere. After the CV scans, the WE was sonicated in CH_2Cl_2 solvent for 10 min to remove the electrolyte and the unreacted or physisorbed **3**, **4a** or **4b**. The WE was further washed with acetone, isopropanol and methanol to obtain the respective grafted monolayers.

Junction and measurement setup

To measure the *I–V* characteristics, a metal/molecule/Si (n++) structure was completed by using a tiny drop of liquid mercury of diameter 600 ± 20 μm as the counter electrode. The contact area in the grafted monolayer was 0.18 ± 0.002 mm^2. The *I–V* curves were recorded at room temperature in a dark box using a pAmeter–dc voltage source (HP 4140).

Theoretical calculation

The ground state geometry optimization and molecular orbitals calculations of the molecules **3**,**4a** and **4b** were done using *ab-initio* molecular orbital theory based LCAO-MO approach as implemented in the GAMESS software. The ionic optimization of the molecules was carried out without any symmetry constraint at the B3LYP/6-31G (d,p) level of theory.

Conclusions

Overall, we have synthesized three alkenylated polyaromatic molecules *viz*. a C-11-perylene (**3**), and the C-6- and C-11-pyrenes (**4a** and **4b** respectively) as prototype σ–π systems, and electro-grafted them individually on H-terminated Si surfaces to form monolayers. The *I–V* characteristics of the monolayers revealed pronounced current rectification in the positive bias. To the best of our knowledge such high RR values are rare except for some devices constructed by Whitesides' group.[41,42] Previously the σ–π systems were attached to silicon wafers by silanization of native oxide with n-alkenyl-trichlorosilane,[11,12] but those devices produced much less RR (~35). Because the attachments were through the strong Si-O-Si linkages (Si-O ~108 kcal mol^{-1}),[54] it would rigidize the molecular assemblies on the surface. This may prevent proper stacking, creating voids and resulting in poor RR values. In comparison, our devices were built through Si-C bonds (Si-C ~76 kcal mol^{-1}), as confirmed from the XPS data. Hence, it is expected to offer more flexibility to the molecules on the Si-surface for more van der Waals interactions ensuring better packing and rectification. As we have prepared only three molecular devices, any attempt to establish the structure-property relationship will be highly speculative. Between the pyrene compounds, the C6-derivative **4b** showed better performance than the C6-derivative **4a**. We did not prepare any device with the C6-derivative of perylene, because our results showed that the alkyl-perylene **3** did not furnish orderly packed monolayers due to the inherent non-planarity of the moiety.

Notes and references

a] *Dr. Kavita Garg, Prof. Sandip K. Nayak, Prof. Subrata Chattopadhyay*
Bio-Organic Division,
Bhabha Atomic Research Centre, Mumbai, India
Email: kavitachemistry1@gmail.com
schatt@barc.gov.in
[b] *Dr. ChiranjibMajumder*
Chemistry Division,
Bhabha Atomic Research Centre, Mumbai, India
[c] *Prof. Dinesh K. Aswal, Prof. Shiv K. Gupta*
Chemistry Division,
Bhabha Atomic Research Centre, Mumbai, India

1. R. M. Metzger, *Acc. Chem. Res.* 1999, **32**, 950–957.
2. W. B. Davis, W. A. Svec, M. A. Ratner, M. R. Wasielewski, *Nature* 1998, **39**, 660–63.
3. C. Joachim, J. K. Gimzewski, A. Aviram, *Nature* 2000, **408**, 541–548.
4. A. Ulman, *An introduction to ultrathin organic flms: From Langmuir-Blodgett to self-assembly* , Academic Press, Boston, 1991.
5. F. Schreiber, *Prog. Surf. Sci.* 2000, **65**, 151–256.
6. A. Salomon, D. Cahen, S. M. Lindsay, J. Tomfohr, V. B. Engelkes, C. D. Frisbie, *Adv. Mater.* 2003, **15**,1881–1890.
7. D. K. Aswal, S. Lenfant, D. Guerini, J. V. Yakhmi, D. Vuillaume, *Anal. Chim. Acta* 2006, **568**, 84–108.
8. D. Vuillaume, S. Lenfant, D. Guerini, C. Delerue, C Petit, G. Salace. *Pramana J. Phys.* 2006, **1**, 17–32.
9. A. Martiny, J. R. Sambles. *Nanotech.* 1996, **7**, 401–405.
10. A. C. Brady, B. Hodder, A. S. Martin, J. R. Sambles, C. P. Ewels, R. Jones, P. R. Briddon, A. M. Musa, C. A. Panetta, D. L. Mattern, *J. Mater. Chem.* 1999, **9**,2271–2275.
11. J. Chen, W. Wang, M. A. Reed, A. M. Rawlett, D. W. Price, J. M. Tour, *Appl. Phys. Lett.* 2000, **77**, 1224–1226.
12. S. Lenfant, C. Krzeminski, C. Delerue, G. Allan, D. Vuillaume, *NanoLett.* 2003, **3**, 741–746.
13. H. Langhals, S. Demmig, T. Potrawa, J. Prakt. *Chem.* 1996, **333**, 733–748.
14. K. D. Belfield, K. J. Schafer, M. D. Alexander, Jr., *Chem. Mater.* 2000, **12**, 1184–1186.
15. L. D. Wescott, D. L. Mattern, *J. Org. Chem.* 2003, **68**, 10058–10066.
16. J. M. Buriak, *Chem. Rev*. 2002, **102**, 1271−1308.
17. S. Ciampi, J. B. Harper, J. J Gooding, *Chem. Soc. Rev*. 2010, **39**, 2158−2183**.**
18. H. Haick, D. Cahen**,** *Acc. Chem. Res*. 2008, **41**, 359–366.
19. A. Vilan, O. Yaffe, A. Biller, A. Salomon, A. Kahn, D. Cahen, *Adv. Mater*. 2010, **22**, 140–159.
20. A. B. Sieval, A. L. Demirel, J. W. M. Nissink, M. R. Linford, J. H. van der Maas, W. H. de Jeu, H. Zuilhof, E. J. R. Sudhölter, *Langmuir* 1998, **14**, 1759–1768.
21. J. Terry, M. R. Linford, C. Wigren, R. Cao, P. Pianetta, C. E. D. Chidsey, *Appl. Phys. Lett*. 1997, **71**, 1056–1058.
22. M. P. Stewart, J. M. Buriak, *Angew. Chem., Int. Ed*. 1998, **37**, 3257–3260.
23. C. Vieillard, M. Warntjes, F. Ozanam, J. -N. Chazalviel, *Proc. Electrochem. Soc*. 1996, 95, 250–258.
24. E. G. Robins, M. P. Stewart, J. M. Buriak, *J. Chem. Soc., Chem. Commun*. 1999, 2479–2480.
25. J. M. Buriak, M. J. Allen, *J. Am. Chem. Soc*. 1998, **120**, 1339–1340.
26. M. R. Linford, P. Fenter, P. M. Eisenberger, C. E. D. Chidsey, *J. Am. Chem. Soc*. 1995, **117**, 3145–3155.
27. A. Bansal, X. Li, I. Lauermann, N. S. Lewis, S. I. Yi, W. H. Weinberg, *J. Am. Chem. Soc*. 1996, 118, 7225–7226.
28. D. K. Aswal, S. P. Koiry, B. Jousselme, S. K. Gupta, S. Palacin, J. V. Yakhmi, *Physica E* 2009, **41**, 325–344.
29. S. Lenfant, D. Guerin, F. Tran Van, C. Chevrot, S. Palacin, J.P. Bourgoin, O. Bouloussa, F. Rondelez, D. Vuillaume, *J. Phys. Chem. B* 2006**,** **110**, 13947–13958.
30. Y. Li, S. Calder, O. Yaffe, D. Cahen, H. Haick, L. Kronik, H. Zuilhof, *Langmuir* 2012, **28**, 9920–9929.
31. D. Appelhans, D. Ferse, H.-J. P. Adler, W. Plieth, A. Fikus, K. Grundke, F. -J. Schmitt, T. Bayer, B. Adolphi, *Coll. Surf. A* 2000, **161**, 203–212.
32. L. Scheres, R. Achten, M. Giesbers, L. C. P. M. de Smet, A. Arafat, E. J. R. Sudhölter, A. T. M. Marcelis, H. Zuilhof, *Langmuir* 2008, **25**, 1529−1533.
33. E. Clar, *Polycyclic hydrocarbons*, Academic Press, New York, 1964, Vol II.
34. S. Sankaranarayanan, A. Sharma, B. A. Kulkarni, S. Chattopadhyay, *J. Org. Chem.* 1995, **60**, 4251–4254.
35. J. P. Rabe, S. Buchholz, *Science* 1991, **253**, 424–427.
36. R. Hentschke, B. L. Schürmann, J. P. Rabe, *J. Chem. Phys.* 1992, **96**, 6213–6221.
37. J. Taylor, H. Guo, J. Wang, *Phys. Rev. B.* 2001, **63**, 245407-1–245407-13.
38. R**.** L**.** Cicero, M**.** R**.** Linford, C**.** E**.** D. Chidsey, *Langmuir* 2000, **16**, 5688–5695**.**
39. X. H. Qiu, C. Wang, Q. D. Zeng, B. Xu, S. X. Yin, H. N. Wang, S. D. Xu, C. L. Bai, *J. Am. Chem. Soc.* 2000, **122**, 5550–5556.
40. T. -W. Kim, G. Wang, H. Lee, T. Lee, *Nanotechnol.* 2007, **18**, 315204 (8 pages).
41. C. A. Nijhuis, W. F. Reus, J. R. Barber, M. D. Dickey, G. M. Whitesides, *NanoLett.* 2010, **10**, 3611–3619.
42. C. A. Nijhuis, W. F. Reus, G. M. Whitesides, *J. Am. Chem. Soc.* 2009, **131**, 17814–17827.
43. G. J. Ashwell, D. S. Gandolfo, *J. Mat. Chem*. 2001, **11**, 246–248.
44. J. W. Baldwin, R. R. Amaresh, I. R. Peterson, W. J. Shumate, M. P. Cava, M. A. Amiri, R. Hamilton, G. J. Ashwell, R. M. Metzger, *J. Phys. Chem. B* 2002, **106**, 12158–12164.
45. R. M. Metzger, J. W. Baldwin, W. J. Shumate, I. R. Peterson, P. Mani, G. J. Mankey, T. Morris, G. Szulczewski, S. Bosi, M. Prato, A. Comito, Y. Rubin, *J. Phys. Chem. B* 2003, **107**, 1021–1027.
46. R. M. Metzger, *Chem. Phys*. 2006, **326**, 176–187.
47. G. J. Ashwell, B. Urasinska, W. D. Tyrrell, *Phys. Chem. Chem. Phys.* 2006, **8**, 3314–3319.
48. S. P. Koiry, P. Jha, D. K. Aswal, S. K. Nayak, C. Majumdar, S. Chattopadhyay, S. K. Gupta, J. V. Yakhmia *Chem. Phys. Lett*. 2010, **485**, 137–141.
49. C. Krzeminski, G. Allan, C. Delerue, D. Vuillaume, R. M. Metzger, *Phys. Rev. B* 2001, **64**, 085405.
50. S. Datta, W. Tian, S. Hong, R. Reifenberger, J. I. Henderson, C. P. Kubiak, *Phys. Rev. Lett.* 1997, **79**, 2530-2533
51. A. Aviram, M. A. Ratner, *Chem. Phys. Lett.* 1974, **29**, 277–283.
52. M. V. Skorobogatyi, A. A. Pchelintseva, A. L. Petrunina, I. A. Stepanova, V. L. Andronova, G. A. Galegov, A. D. Malakhov, V. A. Korshun, *Tetrahedron* 2006, **62**, 1279–1287.
53. I. V. Grechishnikova, L. B. A. Johansson, J. G. Molotkovsky, *Chem. Phys. Lipids* 1996, **81**, 87–98.
54. J. M. Tour, *Acc. Chem. Res.* 2000, **33**, 791–804.